Numerical Analysis of Masonry-Infilled Reinforced Concrete Frames

Ibrahim AL-Shaikh [(1)] , Nabil Falah[(2)]

Abstract

Analytical studies have been conducted to investigate the performance of masonry infill reinforced concrete frames under in-plane lateral loading. In this paper, the experimental results were summarized in concisely, and a constitutive model is presented for the modeling masonry units, mortar, and the masonry units/mortar interface in general. 3D finite element models of reinforced concrete frames have been constructed by ABAQUS software. The concrete damaged plasticity model provided by ABAQUS is used to simulate the behavior of concrete. A comparison was performed between the numerical modeling results and the experimental results, to verify that the finite element models in ABAQUS are capable of simulating similar behavior to experimental models. There is good agreements between experimental and numerical results.

Keywords: **Reinforced concrete; Infilled frames; Concrete damaged plasticity; Interface element; Finite element; ABAQUS**

1. Introduction

The general codes does not take into account the performance of masonry infill reinforced concrete frames during the design of these frames and usually fills these frames by masonry walls, and are often neglected in the design phase [1]. Where is considered this kind of elements architectural elements and of non-structural [2,3].

Un-reinforced masonry buildings are designed and constructed only for gravity forces and not for lateral forces. Some conventional designs of un-reinforced masonry structures have shown acceptable performance during past earthquakes in previous periods, where masonry structures are used significantly in Yemen.

(1) Master student, Civil Engineering Department, Faculty of Engineering, University of Science and Technology, Yemen. Email: . ibrahimalshaikh86@gmail.com

(2) Assistant Professor, Civil Engineering Department, Faculty of Engineering, Sana'a University, Yemen. Email: *nabilfalah@hotmail.com*

These structures respond to the stress of the earthquake by working along the joints between infill and confinement elements, the straining and sliding of masonry and confining elements dissipates a significant amount of energy during an earthquake [4].

Infill walls increase the lateral stiffness of the frames, and be as a means of transport interior horizontal forces, on the other hand, the infill walls effect the behavior of the frame where these walls working to reduce the deformations [1].

The experimental test consisted of five reinforced concrete (RC) frames specimens tested under substantial drift-lateral deflection/story height (9%) to study the behavior of failure and deformation for the specimens by Ghassan Al-Chaar et al [5]. Comparisons have been performed between the numerical modeling results and the experimental results, to verify that the finite element models are capable of simulating similar behavior to experimental results.

2. Experimental Program

The test consisted of five RC frames specimens tested under substantial drift-lateral deflection/story height (9%) to study the behavior of failure and deformation for the specimens [5].

The five specimens have been construction with scaling factor 1:2 due to the limitation of the research. The five specimens were all single-story and constructions with different number bays single, double and triple. Material properties of all experimental models are shown in Table 1.

Table 1 Material property of all experimental models [5]

Material	Properties
Concrete	Poisson ratio = 0.2
	Compressive strength = 38.438 MPa
	Modulus of elasticity = 29992 MPa
	Density = 2.4 e^{-9} ton/mm^3
Block	Poisson ratio = 0.15
	Compressive strength = 12.907 MPa
	Modulus of elasticity = 15275.362 MPa
	Density = 1.6 e^{-9} ton/mm^3
Reinforcing steel	Poisson ratio = 0.3
	Yield stress = 338.5 MPa
	Modulus of elasticity = 200000 MPa
	Density = 7.8 e^{-9} ton/mm^3

The distance between column centerlines is 2,032 mm (bay widths), and the rectangular columns size are 203x127 mm and 197 x 127 mm for beams. The infill wall built from a concrete masonry unit, all infill specimens had an aspect ratio (*h*/*w*) of 0.75, and with a slenderness ratio (*h*/*t*) of 13.9. The frames were 1,524 mm in the high. The reinforcement details for all specimens were shown in Figure 1.

3. Numerical Modeling

The most practical way to analysis a structure consisting a large number of degrees of freedom is the finite element method. It can be performed finite element analysis by a number of commercial programs. In this research was used the nonlinear finite element program ABAQUS. That is provision time and cost to conduct experiments in the laboratory.

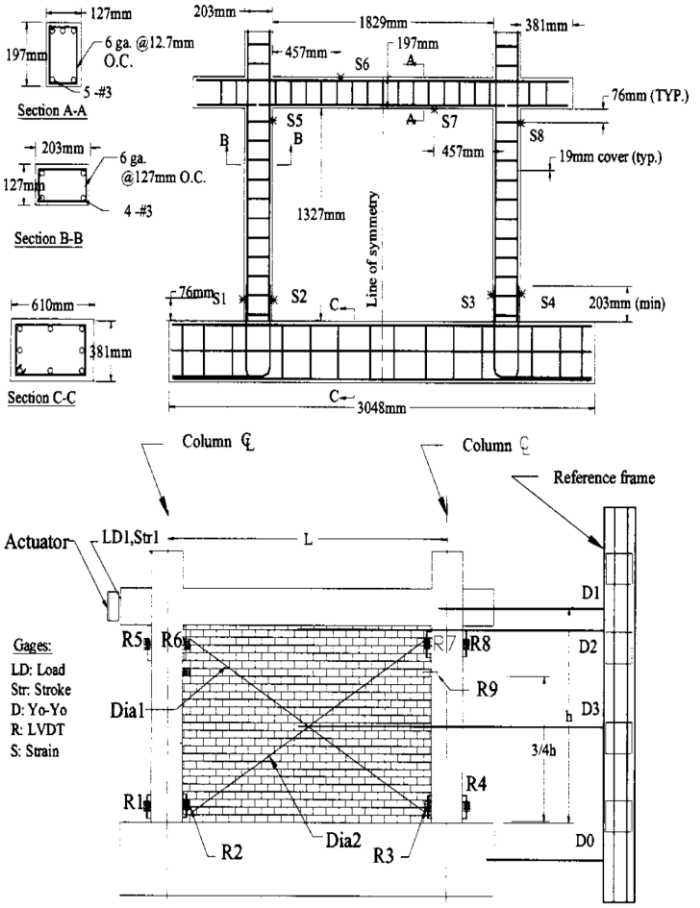

Figure 1 The reinforcement details for all specimens (Ghassan Al-Chaar et al. 2002)

A 3D finite element model of reinforced concrete frames with and without infill walls has been constructed in ABAQUS/Standard 6.12 according to Ghassan Al-Chaar et al. [5] as shown in Figure 2.

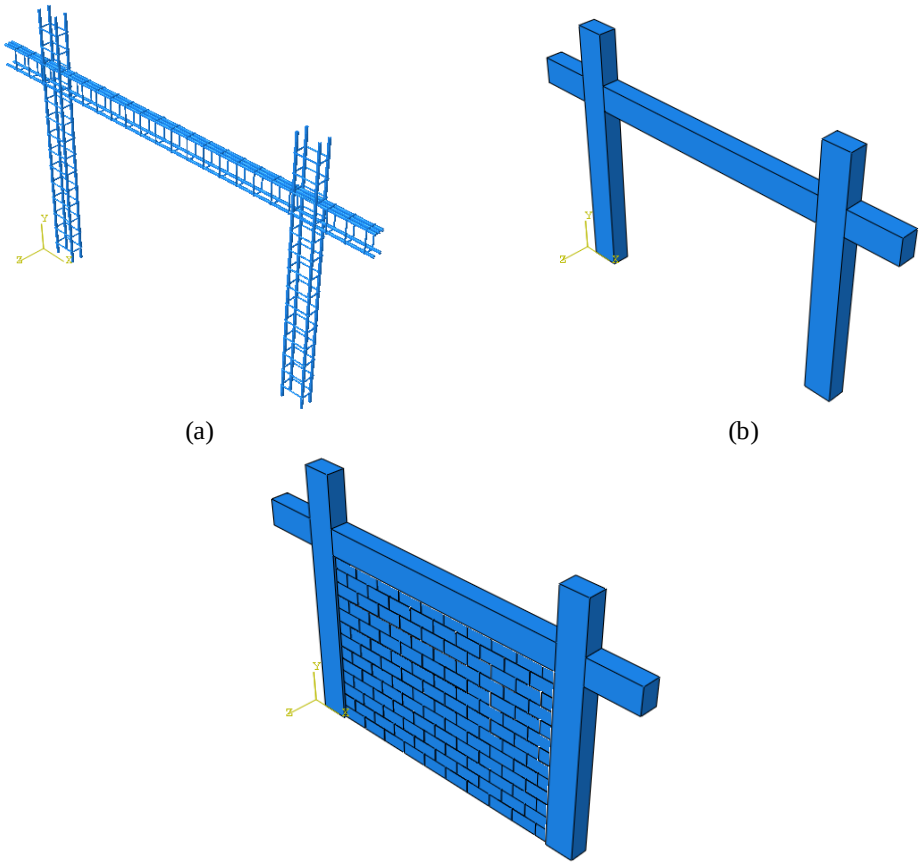

(a) (b)

(c)

Figure 2 The finite element model details (a) Longitudinal and transverse reinforcement (b) Bare frames (c) Infilled frames

3.1 Materials

3.1.1 Concrete

The plastic-damage model in ABAQUS is used to simulate the behavior of concrete in columns, beams and concrete masonry unit. That is based on the proposed models by J. Lubliner et al. [6] and By Jeeho Lee and Gregory L. Fenves [7], that is capable of predicting the behavior of each of the compressive and tension for concrete under external pressures.

Concrete Damaged Plasticity model uses a yield condition based on the yield function proposed by J. Lubliner et al. [6] and It also includes the modifications proposed by Jeeho Lee and Gregory L. Fenves [7] to calculate different evolution of strength under tension and compression, **p** is the hydrostatic pressure stress and **q** is the Mises equivalent effective stress, Figure 3.

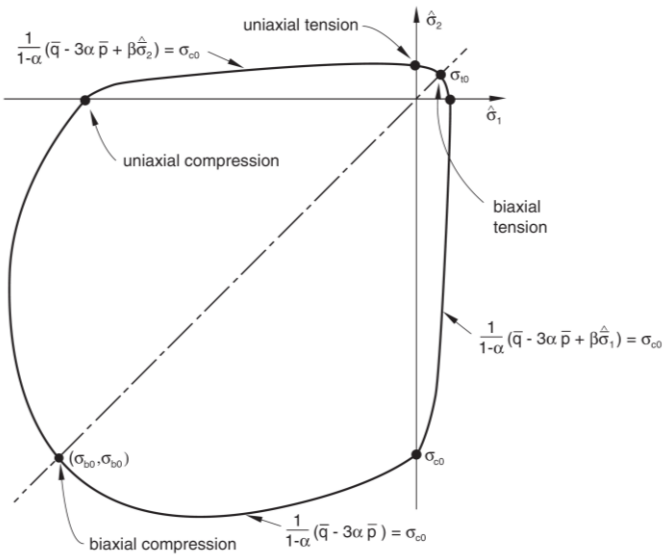

Figure 3 Yield surface in plane stress [8]

The coefficient α can be determined from σ_{b0} the biaxial initial yield compressive stress and σ_{c0} uniaxial initial yield compressive stress, experimental values for stress are $1.10<\sigma_{b0}/\sigma_{c0}<1.16$, yielding values $0.08<\alpha<0.12$ [6], **β** it can be determined from the effective compressive and tensile cohesion stresses.

The damaged in compression and tension are depended on two hardening variables. The hardening variables are equivalent plastic strains in compression $\varepsilon_c^{\sim pl}$ and tension $\varepsilon_t^{\sim pl}$. Crushing and micro-cracking in the concrete model are represented by increasing values of these variables, and the hardening variables control the evolution of the yield surface.

The stress-strain equation for the Concrete Damaged Plasticity is represented by the concept developed by Jeeho Lee and Gregory L. Fenves [7] :

$$\sigma_t = (1-d_t)E_0(\varepsilon_t-\varepsilon_t^{\sim pl}) \qquad 1$$

$$\sigma_c = (1-d_c)E_0(\varepsilon_c-\varepsilon_c^{\sim pl}) \qquad 2$$

The degraded response of concrete is described by $\mathbf{d_c}$ and $\mathbf{d_t}$, which are referred to independent uniaxial damage variables for compression and tension, respectively. Moreover, are assumed to be functions of the temperature, plastic strains, and field variables, and $\mathbf{0 \le d < 1}$.

If $\mathbf{E_0}$ is the initial elastic stiffness for the concrete material, the stress-strain relations under uniaxial compression and tension loading are shown in Figure 4.

The Concrete Damaged Plasticity model is a modification of the Drucker–Prager theory. According to the modifications, the failure surface in the deviatoric plane does not need to be a circle, and it is governed also for parameter **Kc**, Figure 5.

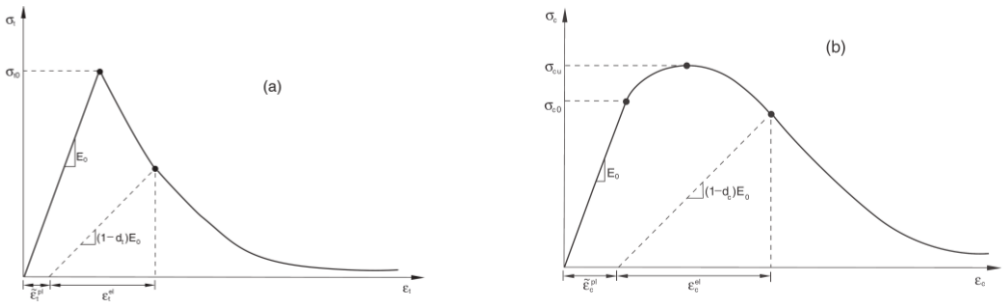

Figure 4 The stress-strain relations for concrete to uniaxial loading (a) In tension (b) In compression. [8]

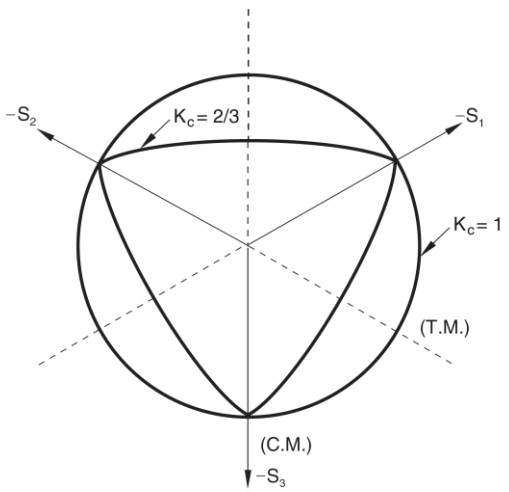

Figure 5 Yield surfaces in the deviatoric plane [8]

The flows potential for Concrete Damaged Plasticity follows the Drucker–Prager hyperbolic are shown in Figure 6. The shape is adjusted through the eccentricity

parameter ϵ , It is a small value that defines the rate of approach of the hyperbola plastic potential to its asymptote. Where ψ is the dilation angle is measured in the **p-q** plane.

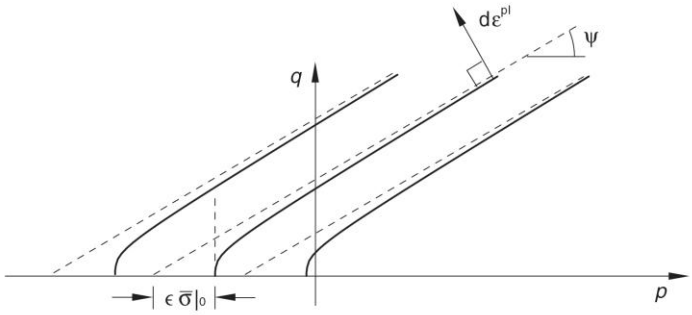

Figure 6 Hyperbolic Drucker–Prager flow potential [8]

The Concrete Damaged Plasticity model in ABAQUS can be regularized using viscoplasticity, therefore allows stresses to be outside of the yield surface, and as can overcome convergence difficulties by defining a small value for viscosity parameter.

The compressive stress-strain curve for the concrete obtained from test experimental conducted by Ghassan Al-Chaar et al. [5], shown in Figure 7.

The stress-strain curve as shown in Figure 8, generally that the tensile stress increases as a straight line with an increase in tensile strain up to the concrete cracking. Then the tensile stress reduces as a straight line to zero. The tensile strength f_{ct} for concrete was calculated equal 10% from compressive strength [9].

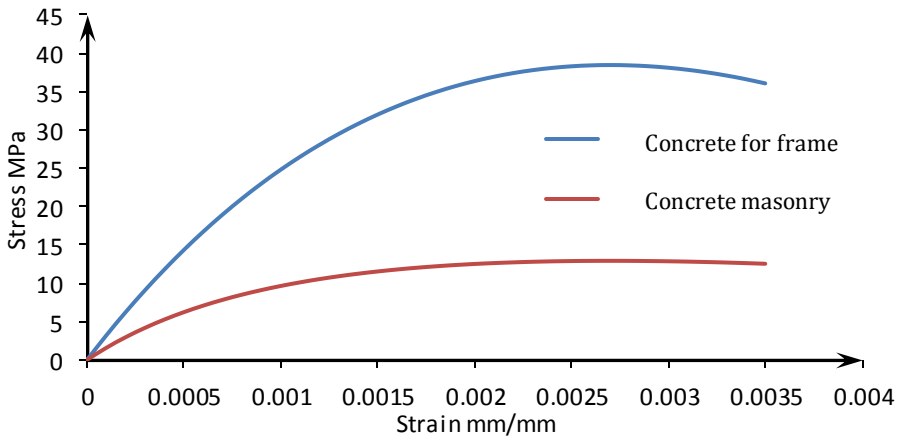

Figure 7 The stress-strain curve for the concrete in compression.

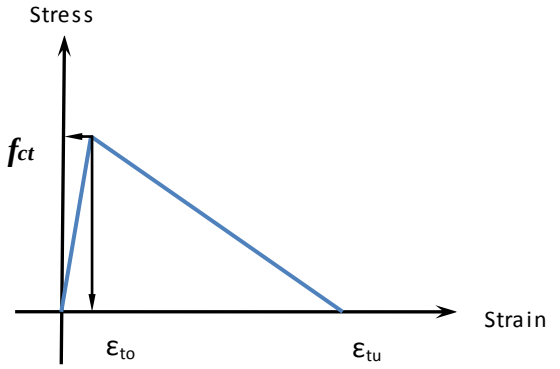

Figure 8 Stress-strain curve for concrete in tension.

The parameters of Concrete Damaged Plasticity that were used for modeling concrete in ABAQUS, are shown in Tables 2.

Table 2 The parameters of Concrete Damaged Plasticity

Dilatation angle	Eccentricity	σ_{b0}/σ_{c0}	K	Viscosity parameter
7	0.1	1.16	0.7	0.00025

3.1.2 Reinforcement Bars

The idealized stress strain curve as shown in Figure 9, would be more appropriate to modeling the behavior of reinforcing steel, the reinforcing steel is modeled as a linear elastic and linear-plastic-hardening material.

The parameters of this model are the stress and strain at the beginning of yielding and the stress and strain at the ultimate load was obtained from experimentally stress-strain relations.

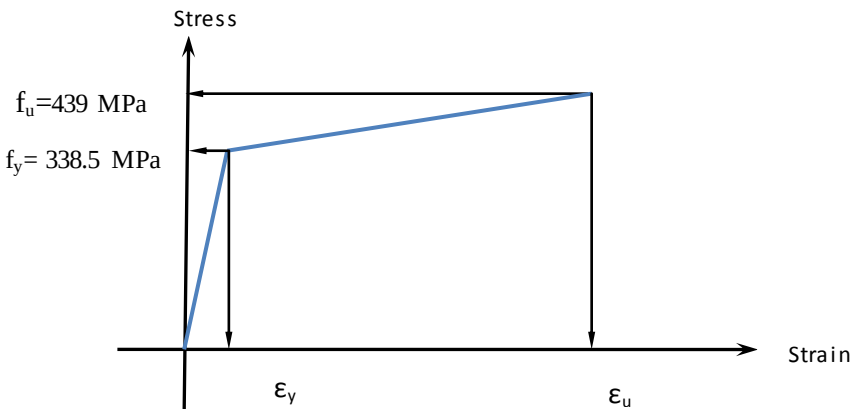

Figure 9 Idealized stress-strain relationship for reinforcing steel material

3.2 Elements Type

The ABAQUS program contains a large number of different element types, categorized based on the aspects that characterize the behavior (family, degrees of freedom, number of nodes, formulation, and integration).

3.2.1 Concrete Elements

The continuum elements in ABAQUS can be used for nonlinear analyses involving plasticity, contact, and large deformations. They are available for stress, heat transfer, coupled thermal-stress, etc. ABAQUS program uses numerical techniques to integrate different quantities over the volume of each the element, therefore allows complete generality in material behavior. It is also uses Gaussian quadrature for most of the elements to evaluate the response of the material at each integration point for each element. Some solid (continuum) elements in ABAQUS can use reduced or full integration, an option which can have an important effect on the accuracy of the elements for a specific problem. Reduced integration reduces the required time for running, especially in three dimensions models. For example, element type C3D20R has only 8 (2x2x2) in each direction integration points, while C3D20 has 27 (3x3x3) integration points, therefore the assembly for element it is approximately 3.5 times lesser for C3D20R than for C3D20, Figure 10. For this research, the C3D8R element, was used to model columns, beams and slabs.

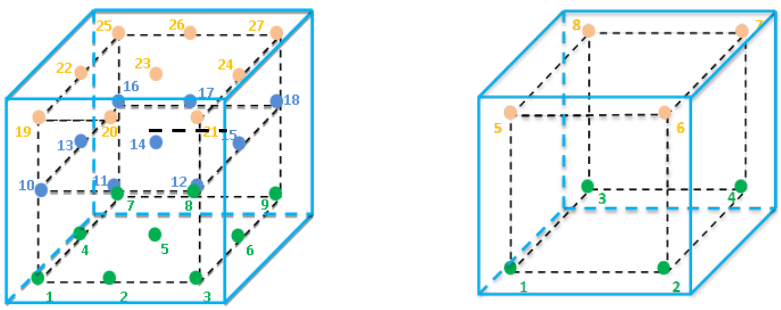

(a) (b)

Figure 10 Integration point for elements (a) C3D20 and (b) C3D20R

3.2.2 Reinforcement Bars Elements

The second type is the truss elements, are used in three or two dimensions to model the slender elements, that support loading only the centerline or along the axis of the element. For this research, the truss element (T3D2) which is used to modeling the reinforcing steel in the members of concrete.

3.2.3 Interface Elements

Masonry wall considered as a composite material that consists from masonry units and mortar joints, Figure 11(a). For a full analysis of the masonry, should be modeling all elements for the masonry (masonry units, mortar, and the masonry units/mortar interface), Figure 11(b). In this way masonry units and mortar in the joints are modeling by continuum elements whereas the unit-mortar interface is modeled by interaction elements. It must be taken into account the following: inelastic properties, the Young's modulus and Poisson's ratio for both masonry unit and mortar. The interface represents the slip plane and potential crack with initial stiffness to prevention interpenetration of the continuum (solid) elements [10].

This enables to study the combined action of unit, mortar and interface. This model for masonry requires large cost and long time to procedure the analysis [10], therefore a simplified micro-modeling of masonry was used in this research, Figure 11(c). In this way masonry units are modeling by continuum (solid) elements, whereas the behavior of the mortar joints and masonry unit/mortar interface is lumped in one interaction element, see Figure 12.

Furthermore we can use the macro-modeling by neglects the difference between masonry units and mortar joints, through taking into account the properties masonry units and mortar joints in an average through homogenization techniques [10], Figure 11(d).

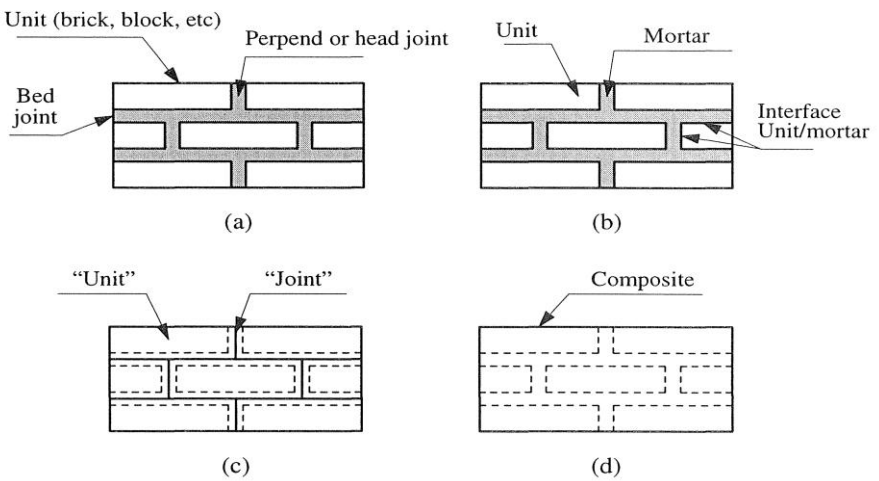

Figure 11 Modeling for masonry structures: (a) Masonry sample (b) Detailed micro-modeling (c) Simplified Micro-modeling (d) Macro-modeling [10]

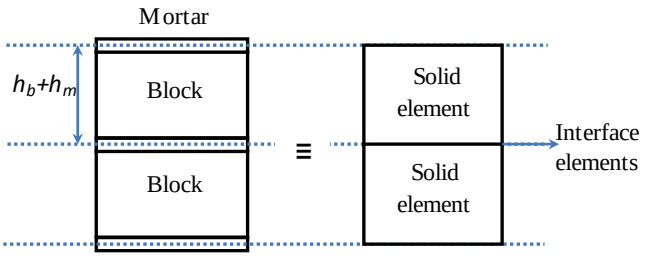

Figure 12 Modeling of simplified micro-modeling for masonry structures with zero thickness elements

The normal and shear stiffness required to define the behavior of mortar joints and masonry unit/mortar interface, can be defined by the following [11]:

$$k_n = \frac{E_u E_m}{h_m(E_u - E_m)} \qquad k_s = \frac{G_u G_m}{h_m(G_u - G_m)} \qquad 3$$

Where k_n and k_s are joint stiffness respectively, for normal and shear, E_u and E_m are modulus of elasticity for unit and mortar, also G_u and G_m are the shear modulus for unit and mortar, and h_m is the actual thickness for the joints. As was also calculate the shear modulus by the following [12]:

$$G = \frac{E}{2(1+\upsilon)} \qquad 4$$

Where E is Modulus of elasticity for unit and mortar, and υ is Poisson's ratio.

To be modeling interface elements in ABAQUS, should be used a specific type of elements that simulate the behavior of the mortar joints. Cohesive elements in ABAQUS are preferable for modeling the behavior of adhesives joints, bonded interfaces.

If the cohesive zone is very thin, and for all practical purposes may be considered to be of zero thickness, the constitutive response is commonly described in terms of a traction-separation law, [8].

The specification of generalized traction-separation behavior for surfaces, this behavior offers capabilities that are very similar to cohesive elements that are defined using a traction-separation law. However, surface-based cohesive behavior is typically easier to define and allows simulation of a wider range of cohesive interactions, [8].

The available traction-separation model in ABAQUS assumes initially linear elastic behavior, followed by the initiation and evolution of damage. The elastic behavior is written in terms of an elastic constitutive matrix that relates the

normal and shear stresses to the normal and shear separations across the interface, [8].

3.3 Constraints & Interactions

3.3.1 Embedded Elements

The ABAQUS provides a large collection of constraints, whereas in this research the embedded elements were used to modeling reinforcing steel in concrete elements, recommended by ABAQUS Manual. Therefore reinforcing steel be embedded in concrete elements (host elements).

The translational degrees of freedom of the embedded node are constrained to the interpolated values of the corresponding degrees of freedom of the host element, [8].

3.3.2 Interactions

Two methods can be used in ABAQUS to modeling the contact. The first method is contact pair, if there are two surfaces that interact with each other. The second method is self-contact if there is single surface that interact with itself, furthermore be used to contact pair to define interactions between bodies. ABAQUS has several contact formulations. Each formulation is based on the number of options a contact discretization, assignment of master and slave roles to the contact surfaces and a tracking approach.

Surface-to-surface discretization considers the shape of both the slave and master surfaces in the region of contact constraints. The surface-to-surface formulation enforces contact conditions in an average sense over regions nearby slave nodes rather than only at individual slave nodes. The averaging regions are approximately centered on slave nodes, with traditional node-to-surface discretization the contact conditions are established such that each slave node on one side of a contact interface effectively interacts with a point of projection on the "master" surface on the opposite side of the contact interface, [8].

A tracking approach will have a considerable effect on how contact surfaces interact. In ABAQUS, there are two tracking approaches to calculation the relative motion for interaction surfaces, the first approach is a finite sliding, it allows any arbitrary motion of the surfaces and which is the most general. The second is small sliding, two bodies may be subjected to large motions, however it assumes there will be relatively little sliding. In ABAQUS cannot be assigned the cohesive

behavior in the contact pairs using the surface-to-surface discretization and the finite sliding tracking approaches.

In this research, a traditional node-to-surface discretization and the small sliding tracking approach was used for modeling the interaction resulting from the mortar which is located between block units.

The choice of master and slave typically has the effect on the results with a node-to-surface contact formulation, see Figure 13.

Generally, if a larger surface contacts with a smaller surface, it is best to choose the larger surface as the master surface and the smaller surface as the slave surface.

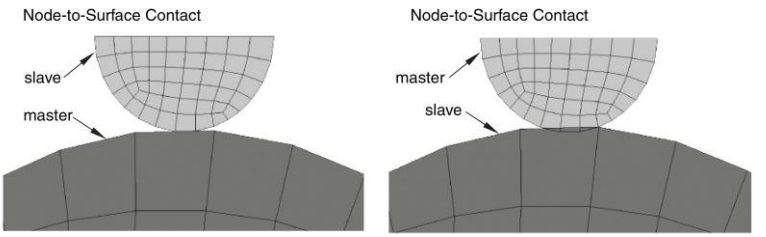

Figure 13 Different master-slave assignments with node-to-surface [8]

3.3.3 Contact Properties

The interaction between surfaces is defined by specify a contact property model for a contact interaction. Mechanical contact property models include, the relationship pressure-overclosure that control the motion of the surfaces, a friction model that specified the resisting tangential motion in the surfaces and a cohesive behavior that allows modeling the behavior of adhesives joints, [8].

The relationship pressure-overclosure was defined in models for this research as the hard contact model. In the hard contact, the penetration is not allowed at each constraint location, there is no end to the magnitude of contact pressure, which can be transferred between the contact surfaces.

To define the friction model between the contact surfaces, must determine the friction coefficient which means that there were shear forces will develop in contact surfaces. For this research, the friction coefficient between concrete masonry units equals 0.44.

Cohesive behavior is defined in ABAQUS as part of the interaction properties that are assigned to the contact surfaces. The properties of interface elements are defined in ABAQUS according to the properties of mortar for the

experimental test of Ghassan Al-Chaar et al. [5], moreover the equations 3 were used to specify the behavior of the interface elements, see Table 3.

Table 3 Interface elements properties for the mortar

k_n (MPa/mm)	k_s (MPa/mm)
16020	11856

3.4 Boundary Condition and Load Application

The nodes at the bottom surface of the two columns in frame are restrained in all degrees of freedom. The load was applied as a lateral deflection at the upper-right of beam as shown in Figure 14.

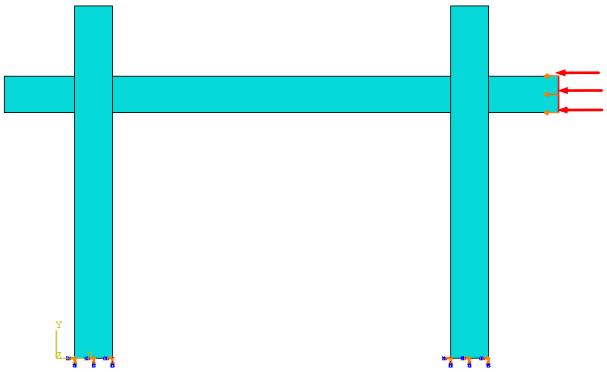

Figure 14. Boundary Condition and Load Application

4. The Results of Numerical

A comparison was performed between the numerical modeling results and the experimental results, to verify that the finite element models in ABAQUS are capable of simulating similar behavior to experimental models.

4.1 Bare-Frame

A 3D finite element model of bare frames has been constructed in ABAQUS according to experimental models [5].

4.1.1 Effect of Mesh Size

In order to evaluation the effects of meshing on the results, three different meshing sizes are followed to procedure numerical analysis the frames, they are:

1. Mesh one: the columns and beam were divided into 100 elements, whereas the reinforcing steel was divided into 326 elements, see Figure 15(a).

2. Mesh two: the columns and beam were divided into 1572 elements, whereas the reinforcing steel was divided into 326 elements, see Figure 15(b).
3. Mesh three: the columns and beam were divided into 1572 elements, whereas the reinforcing steel was divided into 787 elements.

The comparisons of the three meshes are shown in Figure 16. It can be observed, the Mesh three had a good agreement with the experimental results. Depending on a comparison, the Mesh three was selected for modeling all finite element models in the following simulating.

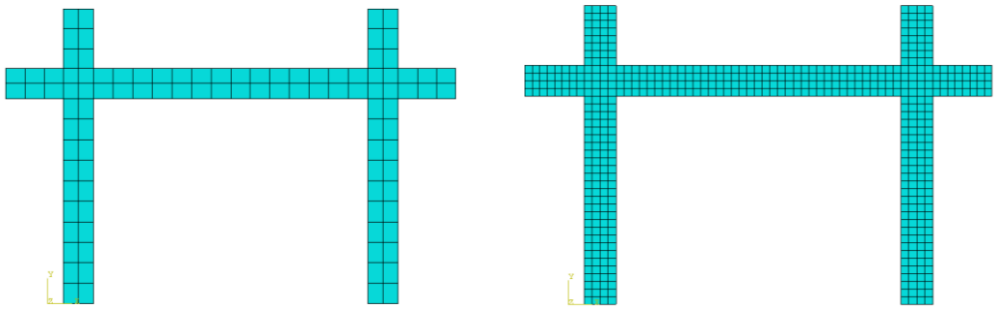

(a) (b)

Figure 15 Different meshes size for concrete (a) Mesh one (b) Mesh two & three.

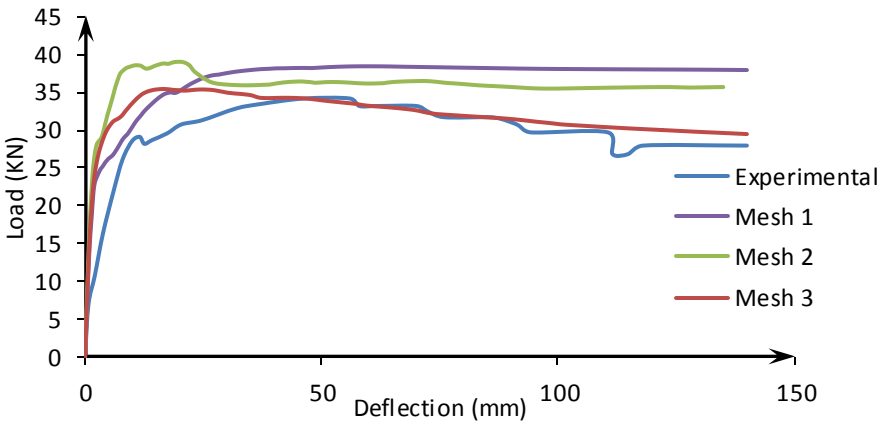

Figure 16 The comparisons between the different meshing sizes.

4.1.2 Effect of Element Type

In addition, in order to evaluation the effect of element types on the results, the element type C3D8 & C3D8R are used to procedure numerical analysis the frames, Figure 17. It can be observed, the element type C3D8 gives close results compared with the experimental results. Furthermore the element

type C3D8R gives a good agreement with the behavior of experimental results, Figure 17.

Depending on a comparison, element type C3D8R was selected for modeling all finite element models in the following simulating. Comparison between deformation in finite element frame and deformation in the experimental frame are shown in Figure 18.

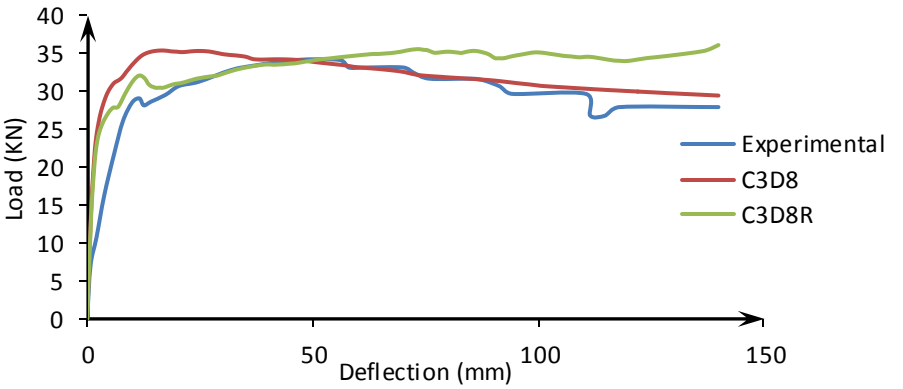

Figure 17 The comparisons between the different element type.

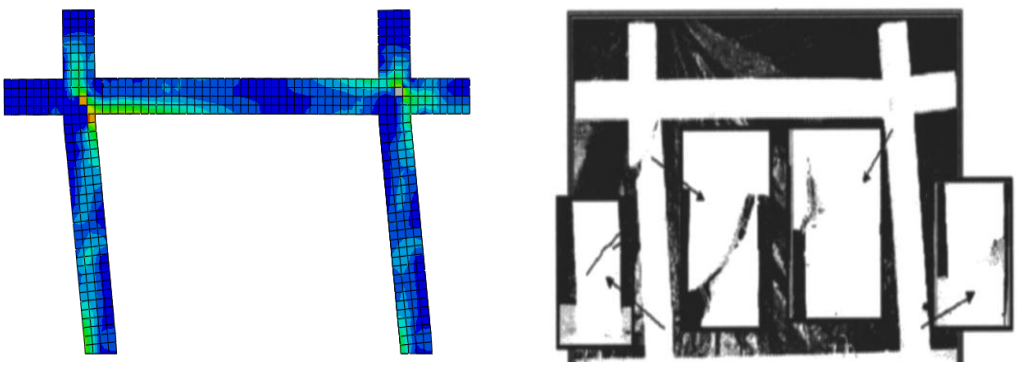

(a) (b)

Figure 18 Comparison between deformations (a) Finite element frame (b) Experimental frame.

4.2 Infilled Frame

A 3D finite element model of infilled frames has been constructed in ABAQUS according to experimental models [5], were selected the element type C3D8R and the same mesh size as the previously. There is a good agreement with the behavior of experimental results as shown in Figure 19.

Comparison between deformation in finite element infilled frame and deformation in experimental infilled frame are shown in Figure 20.

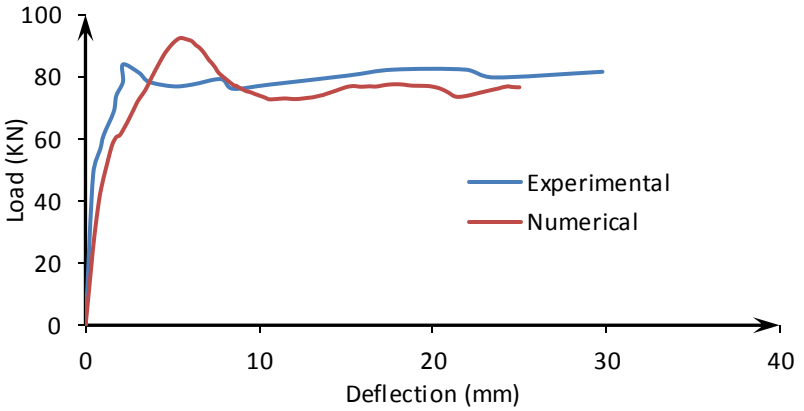

Figure 19 Comparison between finite element infilled frame and experimental infilled frame.

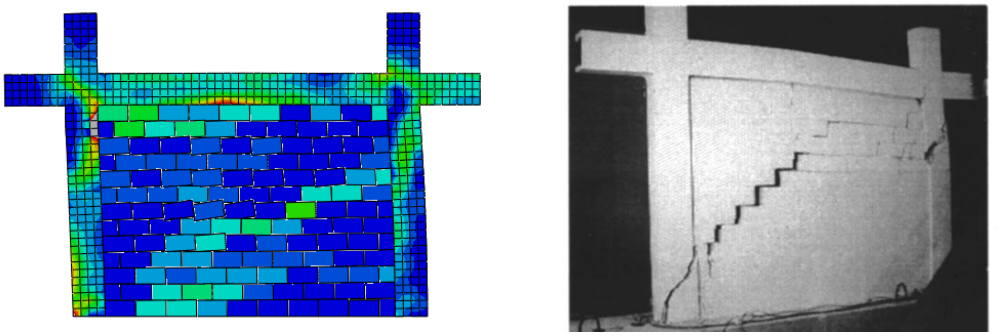

(a) (b)

Figure 20 Comparison between deformations (a) Finite element infilled frame (b) Experimental infilled frame.

5. Conclusions

Depending on comparisons that were performed between the numerical modeling results and the experimental results, it is concluded that:

- The finite element models were able to predict with a good degree of accuracy the behavior of masonry-infilled reinforced concrete frames.
- Meshing sizes have important effect on the behavior of numerical model.
- The use of element C3D8 for modeling frames gives close results compared with the experimental results. Furthermore the use element C3D8R for modeling frames gives a good agreement with the behavior of experimental results.

We recommend researchers to study the effect of the openings and their places in the infill walls.

6. References

[1] Amir Saedi Daryan et al. "A Study of the Effect of Infilled Brick Walls on Behavior of Eccentrically Braced Frames Using Explicit Finite Elements Method" American J. of Engineering and Applied Sciences 2 (1): 96-104 (2009).

[2] J. Centeno et al. "Shake Table Testing Of Gravity Load Designed Reinforced Concrete Frames With Unreinforced Masonry Infill Walls" The 14 th World Conference on Earthquake Engineering ,Beijing China (2008).

[3] M. Lupoae et al. "Aspects Concerning Progressive Collapse of a Reinforced Concrete Frame Structure with Infill Walls" World Congress on Engineering Vol III , WCE 2011, London, U.K (2011).

[4] Samaresh Paikara1 and Durgesh C. Rai "Confining Masonry Using Pre-Cast Rc Element For Enhanced Earthquake Resistance" Proceedings of the 8th U.S. National Conference on Earthquake Engineering, San Francisco, California, USA (2006).

[5] Ghassan Al-Chaar et al. "Behavior of Masonry-Infilled Nonductile Reinforced Concrete Frames" Journal Of Structural Engineering Vol. 128:1055-1063(2002).

[6] J. Lubliner et al "A Plastic-Damage Model for Concrete" International Journal of Solids and Structures, vol. 25, pp. 299–329 (1989).

[7] Jeeho Lee and Gregory L. Fenves "Plastic-Damage Model for Cyclic Loading of Concrete Structures" Journal of Engineering Mechanics, vol. 124, no.8, pp. 892–900 (1998).

[8] Dassault Systèmes. ABAQUS Manual, Version 6.12, 2012.

[9] A.H. Nilson et al. "Design Of Concrete Structures", 14th edition, McGraw-Hill, United States (2010).

[10] Lourenço P.B., Rots J.G., Blaauwendraad J. "Two Approaches For The Analysis of Masonry Structures: Micro And Macro-Modeling", HERON, Vol. 40. No.4, p. 313-340 (1995).

[11] Lourenço, P.B. "Analysis of masonry structures with interface elements", Report No. 03.21.22.0.01, Delft University of Technology, Delft, Netherlands, 72 pp (1994).

[12] T. H. G. Megson "Structural And Stress Analysis", 1st edition, Butterworth-Heinemann, UK (1996).